Title

The crystal structure of oxaliplatin: A case of overlooked pseudo symmetry

Author

Johnstone, Timothy C

Publication Date

2014

DOI

10.1016/j.poly.2013.10.003

Peer reviewed

Published in final edited form as:
Polyhedron. 2014 January 8; 67: . doi:10.1016/j.poly.2013.10.003.

The Crystal Structure of Oxaliplatin: A Case of Overlooked Pseudo Symmetry

Timothy C. Johnstone*
Department of Chemistry, Massachusetts Institute of Technology, Cambridge, MA, 02139

Abstract

The crystal structure of the anticancer drug oxaliplatin, [Pt(*R*,*R*-DACH)(oxalate)] (DACH = diaminocyclohexane), was first reported in the non-centrosymmetric space group $P2_1$, confirming the sole presence of the *R*,*R* enantiomer of the DACH ligand [M. A. Bruck *et al.*, *Inorg. Chim. Acta*, 92 (1984) 279–284]. It was later proposed that the crystal structure is better described in the centrosymmetric space group $P2_1/m$, signifying the presence of the compound as a racemic mixture [A. S. Abu-Surrah *et al.*, *Polyhedron*, 22 (2003) 1529–1534]. Herein is presented a reinvestigation of this crystal structure, which shows that the discrepancy between the two proposed space group assignments arises from overlooked pseudo symmetry. The crystal structures of the synthetic precursor to oxaliplatin, Pt(*R*,*R*-DACH)I_2, and a platinum(IV) derivative, *trans*-[Pt(*R*,*R*-DACH)(oxalate)$(OH)_2$], were also determined, and the absolute configuration of the DACH ligand in each was confirmed to be *R*,*R*. A spectroscopic investigation of the optical rotatory dispersion (ORD) of the oxaliplatin crystals was carried out to further confirm the lack of the true crystallographic mirror plane required for a $P2_1/m$ solution. The ORD was theoretically simulated, in one instance, by applying the Kramers-Kronig transform to the computed circular dichroism spectrum and was found to corroborate the spectroscopic and crystallographic findings. Finally, a brief discussion is given of the importance of discussing the details of nuanced crystal structures and of providing evidence in addition to X-ray structure determination if chemically unexpected results are obtained.

Keywords

Oxaliplatin; X-ray crystallography; pseudo symmetry; optical rotatory dispersion; Kramers-Kronig transform; absolute structure

1. Introduction

Oxaliplatin, Pt(*R*,*R*-DACH)(oxalate) (Fig. 1), is a third generation platinum anticancer agent that is used in combination with 5-fluorouracil and leucovorin for the treatment of metastatic colorectal cancer [1]. This drug, approved by the US Food and Drug Administration in 2004, follows on the success of the other platinum-based drugs cisplatin and carboplatin (Fig. 1), which were approved in the 70s and 80s, respectively [2]. The mechanism of action of cisplatin is comprised of 4 key steps: entry into the cell via active or passive transport,

*Corresponding author: Tel.: (617) 253-1824, Fax: (617) 258-8150, timothyj@mit.edu, Mailing address: 77 Massachusetts Ave., Building 18, Room 443, Cambridge, MA, 02139.

activation/aquation resulting in loss of chloride ligands, binding to DNA, and subsequent cellular processing of the DNA damage, which triggers apoptosis [3]. The key design feature of carboplatin was the replacement of the chloride leaving-group ligands of cisplatin with the chelating cyclobutanedicarboxylate (CBDCA). The development of oxaliplatin varied from that of carboplatin in that both the leaving-group and the non-leaving-group ligands differ from those of cisplatin. The non-leaving-group ligands (Fig. 1) are those that remain bound to the platinum throughout all 4 steps of the mechanism of anticancer action.

One particularly distinguishing characteristic of oxaliplatin is that the chelating *trans*-diaminocyclohexane (DACH) ligand in this compound is enantiomerically pure. The presence of the two chiral centers in DACH allows for the existence of three distinct isomers: *R*,*R*, *S*,*S*, and *R*,*S*. Due to the presence of the chiral carbon atoms within an alicyclic cyclohexane ring, the *R*,*R*, and *S*,*S* isomers necessarily place the amine groups in a trans configuration. In the *R*,*S* isomer, the amines are cis to one another. It was found during the drug development process that the complex containing the *R*,*R* isomer is more potent than that containing the *S*,*S* ligand, a racemic mixture of the two enantiomers, or the *R*,*S* ligand [4]. As a result of the enhanced activity of the *R*,*R* isomer, this enantiomer was carried forward and eventually approved for clinical use. In 1981, the crystal structure of Pt(*trans*-DACH)(oxalate), prepared using enantiomerically pure *R*,*R* diamine ligand as a starting material, was reported [5]. The absolute stereochemistry (*R*) at each of the chiral carbons in the platinum complex was confirmed using the anomalous dispersion of the platinum atoms within the crystal.

It comes as a surprise, then, that the Cambridge Structural Database (CSD) contains a structure of [Pt(*rac*-*trans*-DACH)(oxalate)] that is described as a correction to the original oxaliplatin structure. In the corresponding paper, Abu-Surrah *et al*. state that the original crystallographic result was incorrect and that the crystal structure of oxaliplatin is properly described as a racemic twin that contains both the *R*,*R* and *S*,*S* enantiomers in equal proportion [6]. The authors reach this conclusion solely on the basis of their crystallographic results. From this conclusion, they also draw the corollary that the C–N bonds of the chelating diamine are broken and reformed during the synthesis of oxaliplatin.

It is widely established that oxaliplatin, when prepared using enantiomerically pure ligand, consists of an enantiomerically pure product as can be confirmed, for example, by the optical activity of solutions of the final product [7]. It might, therefore, be tempting to discount the correction to the oxaliplatin structure outright as chemically nonsensical. The crystallographic results presented by Abu-Surrah *et al*. are intriguing, however, in light of the fact that *PLATON* [8, 9] suggests the presence of missed higher symmetry in the structure originally published by Bruck *et al*.

In this paper, a reinvestigation of the crystal structure of oxaliplatin is carried out, which shows that the higher symmetry proposed to be present by Abu-Surrah *et al*. is rather a mistaken case of pseudo symmetry. As further evidence to support this conclusion, the absolute structures of the synthetic intermediate Pt(*R*,*R*-DACH)I_2 and the oxaliplatin derivative *trans*-[Pt(*R*,*R*-DACH)(oxalate)$(OH)_2$] were confirmed crystallographically. Spectroscopic evidence, supported by theoretical calculations, is also presented to confirm the presence of pseudo symmetry in the crystal structure of oxaliplatin. Among the computational results is a prediction of the optical rotatory dispersion of oxaliplatin obtained by application of the Kramers-Kronig transform to the computed circular dichroism spectrum. Finally, a discussion is given of the importance of describing nuanced crystallographic studies and of supporting crystallographic data with supplementary techniques in the event that chemically unintuitive results are obtained.

2. Materials and Methods

2.1. Synthesis

Oxaliplatin [10], Pt(*R*,*R*-DACH)I_2 [11], and *trans*-[Pt(*R*,*R*-DACH)(oxalate)$(OH)_2$] [12] were prepared as previously described. Spectroscopic characterization was consistent with that recorded in the literature.

2.2. X-ray Crystallography

2.2.1. Crystal growth and data collection—Colorless blocks of oxaliplatin were grown by allowing a hot saturated aqueous solution of the complex to cool to room temperature and then letting the solution stand at that temperature for one week. Yellow needles of [Pt(*R*,*R*-DACH)I_2]·DMF were grown by vapor diffusion of diethyl ether into a DMF solution of the complex. Colorless plates of *trans*-[Pt(*R*,*R*-DACH)(oxalate)$(OH)_2$] · $3H_2O$ were grown by allowing a hot aqueous solution of the complex to cool to room temperature overnight. Samples suitable for X-ray diffraction were selected following microscopic examination under crossed polarizers. Crystals were mounted on a nylon cryoloop in Paratone oil and cooled to 100 K under a stream of nitrogen. A Bruker APEX CCD X-ray diffractometer controlled by the *APEX2* software was used to record the diffraction of graphite-monochromated Mo Kα radiation (λ = 0.71073 Å) [13]. The data were integrated with *SAINT* [14] and absorption, Lorentz, and polarization corrections were calculated by *SADABS* [15].

2.2.2. Solution and refinement of the structure of oxaliplatin—In order to fully justify the solution that will be presented here, the steps of the structure solution and refinement will be described in greater detail than is typically common. As will be discussed in Section 3.4, in nuanced instances such as this, a detailed explanation of the reasons that a particular solution was chosen and that others were rejected could avoid unnecessary reevaluations.

Indexing the diffraction pattern of the oxaliplatin crystal with *APEX2* provided a unit cell with metric symmetry that could correspond to either the orthorhombic or monoclinic (β = 90.3°) crystal systems. An examination of the diffraction pattern showed the Laue symmetry to be 2/m and indicated which angle was the correct β. Integration of the data using this setting also provides better merging R-values than those obtained using another angle as β or the orthorhombic crystal system. This fortuitous approach of β to 90° appears to be unrelated to the pseudo symmetry that will be discussed below. The systematic absences do not indicate any centering but do reveal the presence of a 2_1 screw axis and the absence of any glide planes. The intensity distribution within the diffraction pattern [16] suggests that the structure is non-centrosymmetric with $\langle E^2 - 1 \rangle = 0.658$. Although not conclusive, this result suggests that the correct space group is $P2_1$ and not $P2_1/m$.

The initial solution in $P2_1$ via direct methods revealed the locations of the platinum atom, the atoms of the oxalate ligand, and the nitrogen atoms of the DACH ligand. Subsequent refinement produced a difference map in which the residual electron density peaks resembled a cyclohexane ring disordered across the two orientations that would correspond to *R*,*R*- and *S*,*S*-DACH. Carbon atoms were assigned so as to give the *R*,*R* isomer. Hydrogen atoms were placed at calculated positions and refined using a riding model with U_{iso}=1.2U_{iso} of the atom to which they are attached. Anisotropic refinement of the thermal displacement parameters of all non-H atoms, correction for extinction, and adjustment of the weighing scheme to convergence resulted in a model with no significant residual electron density and R_1 = 1.11%. The thermal displacement parameters of two pairs of carbon atoms,

one in the oxalate ligand and one in the cyclohexane ring, were constrained to be equal. The use of this constraint is justified in Section 3.1.

The Flack *x* parameter [17] refined to a value of 0.035(11). The complementary Hooft *y* parameter [18] was calculated to be 0.033(7). Due to the fact that the *hole-in-one* algorithm employed by *SHELXL97* does not simultaneously and jointly refine the Flack *x* parameter along with all other parameters, refinement of the structure as a racemic twin was carried out [19]. The batch scale factor of the second twin domain refined to a value of less than 5%. Furthermore, the Baysian statistical analysis of Hooft, Straver, and Spek, implemented in *PLATON* [18], also predicts that the structure has the correct absolute configuration ($P3_{true}$ = 1.000) and that there is no probability of the structure being a racemic twin ($P3_{rac\text{-}twin}$ = 0.000). Similar results are obtained regardless of whether a Gaussian or a Student's *t*-distribution is used [20]. For the sake of completeness, the structure was also fully refined in $P2_1/m$. The refinement was stable, but resulted in a higher R_1 value of 1.22% and the first component of the weighing scheme refined to a value of zero. The structure in $P2_1$ was validated using *PLATON* and *checkCIF*. The only significant alert arose from the presence of the pseudo mirror plane resulting in the suggestion of $P2_1/m$ as a potential space group. A more detailed comparison of the results from the different refinements is presented in Section 3.1.

2.2.3. Crystal structure of [Pt(R,R-DACH)I_2] ·DMF—The metric symmetry of the unit cell indicates that the crystal system is triclinic. The initial solution with direct methods was carried out in P1 because the ligand is expected to be enantiomerically pure. The heavy atoms were located for the two independent molecules in the unit cell and subsequent refinement cycles revealed the positions of the remaining non-hydrogen atoms. The stereochemistry of the DACH ligands in both of the independent molecules was *R*,*R*. Non-hydrogen atoms were refined anisotropically and hydrogen atoms were treated as described above with the exception that, for the hydrogen atoms of terminal methyl groups, U_{iso}=1.5U_{iso} of the atom to which the hydrogen atoms are attached. In order to obtain a satisfactory final refinement, the DMF molecules of crystallization were constrained to have identical thermal displacement parameters. The Flack *x* parameter refined to 0.027(6). Refinement as a racemic twin resulted in a batch scale factor of 3.4% for the second twin domain. The structure of Pt(*R*,*R*-DACH)I_2 without any solvent of crystallization has also been reported [11]. The geometries of the platinum complexes from the two structures are highly similar and demonstrate a root-mean-squared deviation in non-H atomic positions of 0.036 Å.

2.2.4. Crystal structure of trans-[Pt(R,R-DACH)(oxalate)($OH)_2$] · 3H_2O—The metric symmetry of the unit cell and the Laue symmetry of the diffraction pattern are consistent with the orthorhombic crystal system. The systematic absences are uniquely consistent with the space group $P2_12_12_1$. The solution was obtained using direct methods and refinement was carried out as for the structures above with the exception that the positions of the hydrogen atoms on the waters of crystallization and the coordinated hydroxide ligands, all located in difference Fourier maps, were restrained to 0.82(2) Å. The final positions of the hydrogen atoms were consistent with a hydrogen-bonding network that extends through the crystal. The Flack *x* parameter refined to a value of 0.003(5).

2.2.5. Optical Rotatory Dispersion—A sample of crystalline oxaliplatin (2 mg) was ground with potassium bromide (100 mg) and pressed into a transparent pellet. The pellet was placed in the optical path of a Jasco model 1010 polarimeter and optical rotation was measured in degrees. The wavelength of optical rotation was selected by using filters that

permit transmission of light at 589 nm, 577 nm, or 435 nm. Ten measurements were collected and averaged at each wavelength.

2.2.6. Theoretical calculations—Quantum mechanical density functional theory (DFT) calculations carried out using *ORCA* [21] employed the PBE0 hybrid functional [22] along with the def2-TZVP(-f) Ahlrichs basis set. The zero order regular approximation (ZORA) was used to account for relativistic effects [23] and the resolution of the identify-chain of spheres (RIJCOSX) approximation was used in the evaluation of the Coulomb and exchange matrices [24]. The DFT calculations carried out in *Gaussian03* [25] employed the PBE0 functional as well but used the Pople-type 6-31++g(d,p) basis set for non-platinum atoms and the LANL2DZ effective core potential for the platinum atom [26]. The atomic coordinates from the crystal structure of oxaliplatin reported in this paper were used as the input for geometry optimizations in both *ORCA* and *Gaussian03* with the above-indicated model chemistries, respectively. Frequency calculations were carried out to confirm that each converged upon geometry was at a stationary point on the potential energy surface of the molecule.

Time dependent density functional theory (TDDFT) calculations were carried out in *ORCA* to provide the theoretical circular dichroism (CD) spectrum of the molecule. Since the experimental optical rotation measurement was carried out on a solid sample, no solvation model was incorporated into the calculation. Application of the Kramers-Kronig (KK) transform to the calculated CD spectrum provided theoretical optical rotation values at 589 nm, 577 nm, and 435 nm. The implementation of the KK transform used was based on that described by Polavarapu [27]. Optical rotation was obtained with Equation 1, in which $[\phi(\lambda)]$ is the molar rotation at wavelength λ and $[\theta(\mu_j)]$ is the molar ellipticity at wavelength μ_j. In order to avoid the singularity that would arise at $\lambda = \mu_j$, Polavarapu used an alternating summation. Although the summations performed here span the region in which $\lambda = \mu_j$, the use of alternating summation was unnecessary because conversion of the *ORCA* output from cm^{-1} into nm resulted in a CD spectrum in which none of the discretely computed μ_j values were exactly 589 nm, 577 nm, or 435 nm, which were the λ values evaluated. A normal summation was therefore used.

$$[\phi(\lambda)]=\frac{1}{\pi}\sum_j\left[\frac{[\theta(\mu_j)]}{\lambda-\mu_j}-\frac{[\theta(\mu_j)]}{\lambda+\mu_j}\right] \quad (1)$$

The optical rotation values could also be directly computed using coupled-perturbed Kohn-Sham linear response theory as implemented in *Gaussian03*. The specific rotation of the molecule at the defined wavelengths was the direct output.

3. Results and Discussion

3.1. Crystallography

The crystal structure of oxaliplatin in space group $P2_1$, first reported by Bruck *et al*., confirmed the *R*,*R* stereochemistry of the DACH ligand bound to the platinum atom [5]. In this structure determination, the authors confirmed the stereochemistry using the anomalous scattering of the platinum atoms and report that if the mirror image of the oxaliplatin structure is refined, the R value increases by a factor of 1.08 indicating that the *R*,*R* assignment is correct with a probability of >99.5% [28]. All of the atoms, except the platinum, were refined isotropically and no other comment on the refinement process was given. One telling feature that can be appreciated in their data is the anti-correlation that appears to exist between atoms approximately related by a mirror plane perpendicular to the coordination plane and containing the two-fold molecular symmetry axis (Fig. 2). These

relationships suggest that high correlation matrix elements may exist. As will be described in greater detail below, this correlation is believed to arise from the presence of pseudo symmetry within the crystal.

In 2003, Abu-Surrah *et al*. published a correction to the structure of oxaliplatin [6]. They report that if the structure was solved in $P2_1$, anisotropic refinement resulted in many non-positive definite atoms, whereas solution in $P2_1/m$, with the molecule modeled as a racemate, affords a structure that refines stably. This result is surprising, given the amount of data which have been accrued that indicate that the stereochemistry of the DACH ligand is preserved in the synthesis of oxaliplatin. Their results are also intriguing, given that when the structure deposited in the CSD by Bruck *et al*. is analyzed with *PLATON*, the program suggests the higher symmetry space group $P2_1/m$.

In order to further investigate this phenomenon, a new data set was collected on a crystal of oxaliplatin obtained in the same manner as described by the authors of the previous studies. The structure was refined in $P2_1$ as described in Section 2.2.2. The final model is depicted in Fig. 3 and the refinement parameters are given in Table 1.

These crystallographic data support the choice of $P2_1$ over $P2_1/m$. The anomalous dispersion, used in evaluating both the Flack *x* and Hooft *y* parameters, indicates that the *R*,*R* stereochemistry is correct [29]. It has been noted previously that the Flack *x* parameter can be used to accurately evaluate the absolute structure of pseudo symmetric crystals, provided that a high degree of resonant scattering occurs [30]. Moreover, the Baysian statistical analysis of the differences between the intensities of Bijvoet pairs described by Hooft *et al.*, provides a 0 % probability that the crystal is a racemic twin. These results indicate that the mirror plane introduced on transitioning from $P2_1$ to $P2_1/m$ is not a true crystallographic mirror plane but is rather a pseudo mirror plane and represents an example of global pseudo symmetry. The intensity of the effect of the pseudo symmetry on the structure solution and refinement arises from the dominance of a single heavy atom in the scattering of X-rays from a crystal belonging to a polar space group type. Similar effects have been previously reported for other crystal structures [31–33], and specifically for an instance in which the structure was incorrectly modeled as disordered in a higher symmetry space group [34].

The presence of the pseudo mirror plane introduces correlations between nominally independent parameters and constraints on the similarity of the thermal displacement parameters of some pseudo symmetrically related atoms are required to obtain a satisfactory final solution, as described in Section 2.2.2. As with the structure of Bruck *et al*., *PLATON* suggests the space group $P2_1/m$ on the basis of the symmetry of the atoms within the unit cell, but it can now be recognized that this is only a pseudo space group. The salient differences between the previously published crystal structures, as well as the $P2_1$ and $P2_1/m$ structure from this paper, are collected in Table 2.

The crystal structures of the precursor Pt(*R*,*R*-DACH)I_2 and the derivative *trans*-[Pt(*R*,*R*-DACH)(oxalate)$(OH)_2$] were also investigated. In both cases, anomalous scattering provided a means of confirming the *R*,*R* stereochemistry of the chiral carbon centers of the DACH ligand. Diagrams of the platinum complexes from these two crystal structures are shown in Fig. 4 and selected crystallographic parameters are collected in Table 3.

For all three of the above described structures, the value of the Flack *x* parameter was confirmed by attempting to refine the structure as a racemic twin. In all three cases, the batch scale factor for the second twin component refined to be negligibly small.

3.2. Spectroscopic investigation

Abu-Surrah *et al*. note that crystallization in a centrosymmetric space group could only have arisen if the C–N bonds within the enantiomerically pure ligand employed were broken and reformed. Based on their crystallographic analysis alone, they reached the conclusion that such a racemization must be occurring. Such a proposition should, however, be confirmed by multiple complementary techniques. In this investigation, a spectroscopic experiment was carried out on the oxaliplatin crystals themselves, so as to provide an alternative probe of the solid state structure. Optical rotation was chosen as the spectroscopic handle due to the sensitivity of this technique and the ease of measurement [35]. A suspension of 2 mg of ground crystals in KBr was able to rotate plane polarized light at the sodium D emission line (589 nm) by 0.0357(9)°, a phenomenon that would not have been observed if the structure was a racemic twin. Moreover, a rudimentary evaluation of the optical rotatory dispersion (ORD) of the sample was obtained by also observing an optical rotation of 0.0358(14)° at 577 nm and 0.0976(23)° at 435 nm.

3.3. Theoretical calculations

A TDDFT calculation was carried out using the DFT-optimized geometry of oxaliplatin to simulate the CD spectrum of the molecule (Fig. 5). Using the Kramers-Kronig transform in the manner described in Section 2.2.6, it is possible to compute ORD values at specific wavelengths. On the other hand, the use of linear response theory in conjunction with coupled-perturbed Kohn Sham theory can allow for a direct calculation of optical rotation [36]. Both of these approaches were used to evaluate the optical rotation of oxaliplatin at the experimentally investigated wavelengths. Due to the propensity of *ab initio* calculations to overestimate absolute optical rotation, the experimental and theoretical data were normalized to the rotation at 589 nm. The excellent correlation between the trends present in the experimental and theoretical data is highlighted in Fig. 6.

3.4. Further Comments

The combined results of the experiments described here indicate that the mirror plane identified by Abu-Surrah *et al*. is not a crystallographic mirror plane but is instead a pseudo mirror plane. This pseudo mirror plane is also present in the structure by Bruck *et al*. since these two previous determinations were merely alternate descriptions of the same crystal structure. It is unclear if the presence of the pseudo mirror plane was missed by Bruck *et al*. or if they actively discounted the presence of such a symmetry element for a reason such as the known enantiomeric purity of the DACH starting material and the oxaliplatin product. It can be appreciated in hindsight, however, that an acknowledgement of the presence of the pseudo symmetry element in the original paper would have prevented the faulty correction. A discussion of the pseudo symmetry could also have been used to rationalize the correlations present between the thermal displacement parameters of pseudo symmetrically related atoms.

An additional point to be addressed relates to the use of only crystallographic information to claim that the sample of oxaliplatin had racemized. A large body of literature exists that insists that oxaliplatin can be prepared in an enantiomerically pure form if enantiomerically pure DACH is used. Moreover, chemical reasoning provides no explanation as to how the racemization could occur under the conditions of the reaction or the crystallization. This is not to say that crystallography has not provided chemists with data that causes them to confront unrecognized misconceptions. If strong claims are going to be made based on crystallographic data, however, additional complementary techniques should be used to verify the results obtained from the X-ray structure determination. In this paper, a simple spectroscopic measurement on the crystals themselves demonstrated their ability to rotate plane polarized light. This chiroptical property would not be exhibited by a racemic twin.

4. Conclusion

The original crystal structure of oxaliplatin was published in $P2_1$ and a correction to this structure was published indicating that the correct space group is $P2_1/m$. This change in space group implies that the molecule is a racemate. In this paper, a higher resolution structure is reported. Moreover, a detailed crystallographic analysis and a complementary spectroscopic investigation have been presented that confirm that the original assignment of $P2_1$ is correct. The additional mirror plane that is present in the $P2_1/m$ structure is not a true crystallographic symmetry element, but is rather a pseudo symmetry element. This case highlights the importance of fully describing any nuances that arise during the process of a crystal structure determination so as to prevent future misinterpretations and incorrect reevaluations of structures. This case of overlooked pseudo symmetry also provides a strong rationale for the insistence that crystallographic results that have important chemical implications should be verified by independent and orthogonal physical or chemical means.

Acknowledgments

T.C.J. would like to gratefully thank Prof. S. J. Lippard, not only for the use of laboratory space and his diffractometer, both maintained under CA034992, but also for his encouragement to present these results to the scientific community. The polarimeter is maintained by the MIT Department of Chemistry Instrumentation Facility under NIH grant 1S10RR13886-01.

References

1. Graham J, Muhsin M, Kirkpatrick P. Nat Rev Drug Discov. 2004; 3:11–12. [PubMed: 14756144]
2. Kelland L. Nat Rev Cancer. 2007; 7:573–584. [PubMed: 17625587]
3. Wang D, Lippard SJ. Nat Rev Drug Discov. 2005; 4:307–320. [PubMed: 15789122]
4. Dabrowiak, JC. Metals in Medicine. Wiley; Hoboken: 2009. Platinum Anticancer Drugs.
5. Bruck MA, Bau R, Noji M, Inagaki K, Kidani Y. Inorg Chim Acta. 1984; 92:279–284.
6. Abu-Surrah AS, Al-Allaf TAK, Klinga M, Ahlgren M. Polyhedron. 2003; 22:1529–1534.
7. Noji M, Okamoto K, Kidani Y, Tashiro T. J Med Chem. 1981; 24:508–515. [PubMed: 7241508]
8. Spek AL. J Appl Crystallogr. 2003; 36:7–13.
9. Spek, AL. PLATON, A Multipurpose Crystallographic Tool. Utrecht University; Utrecht, The Netherlands: 2008.
10. Kidani Y, Inagaki K, Iigo M, Hoshi A, Kuretani K. J Med Chem. 1978; 21:1315–1318. [PubMed: 722741]
11. Pažout R, Housková J, Dušek M, Maixner J, Kačer P. Struct Chem. 2011; 22:1325–1330.
12. Zhang JZ, Bonnitcha P, Wexselblatt E, Klein AV, Najajreh Y, Gibson D, Hambley TW. Chem–Eur J. 2013; 19:1672–1676. [PubMed: 23255183]
13. APEX2, 2008-4.0. Bruker AXS, Inc; Madison, WI: 2008.
14. SAINT: SAX Area-Detector Integration Program, 2008/1. University of Göttingen; Göttingen, Germany: 2008.
15. Sheldrick, GM. SADABS: Area-Detector Absorption Correction. University of Gottingen; Gottingen, Germany: 2008.
16. Wilson AJC. Acta Crystallogr. 1949; 2:318–321.
17. Flack HD. Acta Crystallogr Sect A. 1983; 39:876–881.
18. Hooft RWW, Straver LH, Spek AL. J Appl Crystallogr. 2008; 41:96–103. [PubMed: 19461838]
19. Flack HD, Bernardinelli G. J Appl Crystallogr. 2000; 33:1143–1148.
20. Hooft RWW, Straver LH, Spek AL. J Appl Crystallogr. 2010; 43:665–668.
21. Neese F. Wiley Interdiscip Rev: Comput Mol Sci. 2012; 2:73–78.
22. Adamo C, Barone V. J Chem Phys. 1999; 110:6158–6170.
23. Pantazis DA, Chen XY, Landis CR, Neese F. J Chem Theory Comput. 2008; 4:908–919.

24. Neese F, Wennmohs F, Hansen A, Becker U. Chem Phys. 2009; 356:98–109.
25. Frisch, MJ.; Trucks, GW.; Schlegel, HB.; Scuseria, GE.; Robb, MA.; Cheeseman, JR.; Montgomery, J.; Vreven, JAT.; Kudin, KN.; Burant, JC.; Millam, JM.; Iyengar, SS.; Tomasi, J.; Barone, V.; Mennucci, B.; Cossi, M.; Scalmani, G.; Rega, N.; Petersson, GA.; Nakatsuji, H.; Hada, M.; Ehara, M.; Toyota, K.; Fukuda, R.; Hasegawa, J.; Ishida, M.; Nakajima, T.; Honda, Y.; Kitao, O.; Nakai, H.; Klene, M.; Li, X.; Knox, JE.; Hratchian, HP.; Cross, JB.; Adamo, C.; Jaramillo, J.; Gomperts, R.; Stratmann, RE.; Yazyev, O.; Austin, AJ.; Cammi, R.; Pomelli, C.; Ochterski, JW.; Ayala, PY.; Morokuma, K.; Voth, GA.; Salvador, P.; Dannenberg, JJ.; Zakrzewski, VG.; Dapprich, S.; Daniels, AD.; Strain, MC.; Farkas, O.; Malick, DK.; Rabuck, AD.; Raghavachari, K.; Foresman, JB.; Ortiz, JV.; Cui, Q.; Baboul, AG.; Clifford, S.; Cioslowski, J.; Stefanov, BB.; Liu, G.; Liashenko, A.; Piskorz, P.; Komaromi, I.; Martin, RL.; Fox, DJ.; Keith, T.; Al-Laham, MA.; Peng, CY.; Nanayakkara, A.; Challacombe, M.; Gill, PMW.; Johnson, B.; Chen, W.; Wong, MW.; Gonzalez, C.; Pople, JA. Gaussian 03, Revision B.02. Gaussian, Inc; Pittsburgh PA: 2003.
26. Hay PJ, Wadt WR. J Chem Phys. 1985; 82:299–310.
27. Polavarapu PL. J Phys Chem A. 2005; 109:7013–7023. [PubMed: 16834064]
28. Hamilton WC. Acta Crystallogr. 1965; 18:502–510.
29. Flack HD, Bernardinelli G. Chirality. 2008; 20:681–690. [PubMed: 17924422]
30. Flack HD, Bernardinelli G, Clemente DA, Linden A, Spek AL. Acta Crystallogr Sect B. 2006; 62:695–701. [PubMed: 16983149]
31. Murphy VJ, Rabinovich D, Parkin G. J Am Chem Soc. 1995; 117:9762–9763.
32. Murphy VJ, Rabinovich D, Hascall T, Klooster WT, Koetzle TF, Parkin G. J Am Chem Soc. 1998; 120:4372–4387.
33. Kuchta MC, Parkin G. New J Chem. 1998; 22:523–530.
34. Kuchta MC, Dias HVR, Bott SG, Parkin G. Inorg Chem. 1996; 35:943–948. [PubMed: 11666268]
35. Flack HD. Acta Chim Slov. 2008; 55:689–691.
36. Polavarapu PL. Chirality. 2002; 14:768–781. [PubMed: 12395394]

Appendix A. Supplementary data

CCDC 948794, 948795, and 948796 contain the supplementary crystallographic data for oxaliplatin, [Pt(*R*,*R*-DACH)I_2] ·DMF, and *trans*-[Pt(*R*,*R*-DACH)(oxalate)$(OH)_2$] ·$3H_2O$. These data can be obtained free of charge via http://www.ccdc.cam.ac.uk/conts/retrieving.html, or from the Cambridge Crystallographic DataCentre, 12 Union Road, Cambridge CB2 1EZ, UK; fax: (+44) 1223 336 033; or e-mail: deposit@ccdc.cam.ac.uk.

The structure factors for the crystal structures presented here are also provided as supplementary information along with the CIF for the $P2_1/m$ solution of the oxaliplatin structure described in the present work.

Synopsis

The previously reported crystal structures of oxaliplatin have been reevaluated to take into consideration overlooked pseudosymmetry. Crystallographic analysis confirmed the absolute configuration of oxaliplatin, the oxaliplatin precursor Pt(*R*,*R*-DACH)I_2, and the oxaliplatin derivative *trans*-[Pt(*R*,*R*-DACH)(oxalate)$(OH)_2$]. Optical rotatory dispersion measurements and theoretical calculations confirm that the symmetry in the crystal structure is pseudosymmetry.

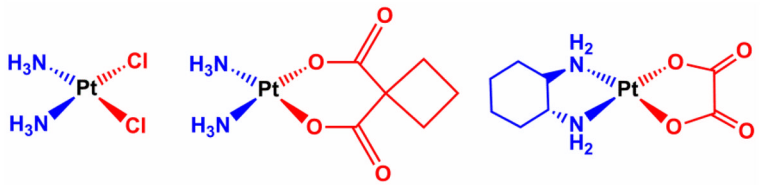

Fig. 1.
The chemical structures of (left to right) cisplatin, carboplatin, and oxaliplatin. The leaving-group ligands are shown in red and the non-leaving-group ligands in blue (color online).

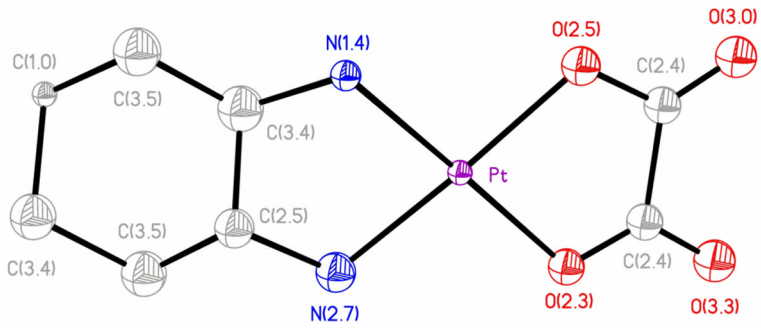

Fig. 2.
Molecular diagram from the crystal structure of oxaliplatin published by Bruck *et al*. The numbers in parentheses are the isotropic Debye-Waller factors for each atom.

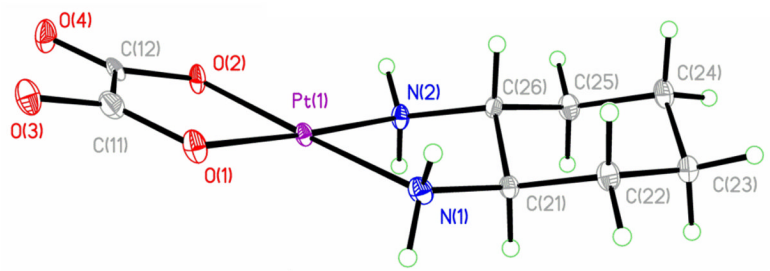

Fig. 3.
Molecular diagram of oxaliplatin with thermal ellipsoids drawn at the 50% probability level.

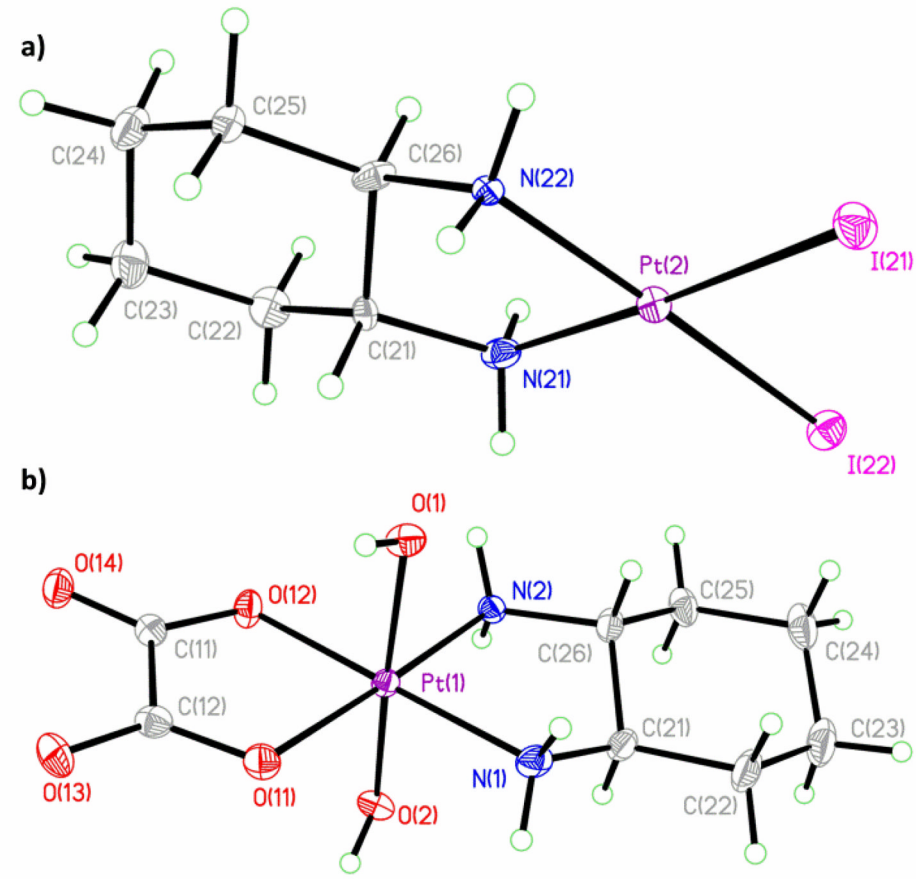

Fig. 4.

Molecular diagrams from the crystal structures of a) Pt(*R*,*R*-DACH)I_2 and b) *trans*-[Pt(*R*,*R*-DACH)(oxalate)$(OH)_2$]. Thermal ellipsoids are drawn at the 50% probability level.

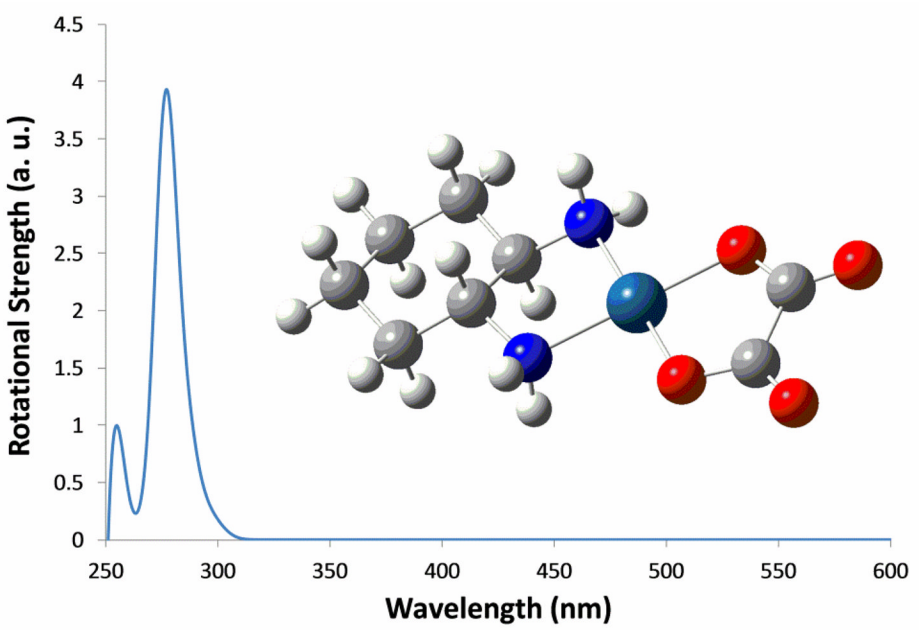

Fig. 5.
Calculated CD spectrum of oxaliplatin. The optimized geometry on which the calculation was carried out is shown as an inset. Color code: O, red; N, blue; C, grey; H, white; Pt, teal (color available online).

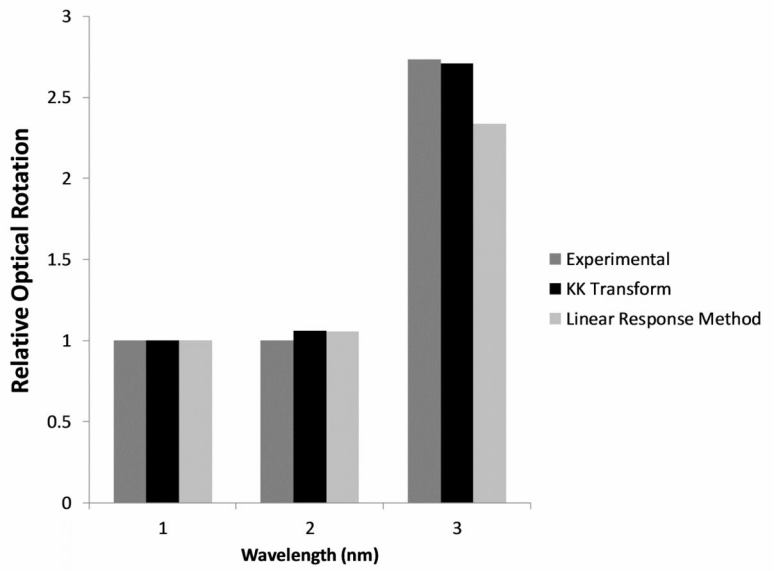

Fig. 6.
Comparison of experimental and theoretically calculated ORD of oxaliplatin. Optical rotation values are normalized to the value at 589 nm.

Table 1

Crystallographic parameters for oxaliplatin

	Oxaliplatin
Formula	$C_8H_{14}N_2O_4Pt$
Formula weight	397.30
Space group	$P2_1$
a, Å	4.6468(2)
b, Å	9.9252(5)
c, Å	11.1991(6)
β, °	90.3130(7)
V, Å^3	516.50(4)
Z	2
T, K	100(2)
μ(Mo Kα), mm^{-1}	13.580
θ range, °	1.82 to 29.60
total no. of data	10941
no. of unique data	2802
no. of parameters	125
completeness to θ (%)	99.8
Flack *x*	0.035(11)
Extinction coeff.	0.0092(3)
R_1[a] (%)	1.11
wR_2[b] (%)	2.71
GOF[c]	1.134
max, min peaks, e Å^{-3}	0.73 and −0.64

[a] $R1=\Sigma||F_O| - |F_C||/ \Sigma|F_O|$.

[b] $wR2= \{\Sigma[w(F_O^2-F_C^2)^2]/\Sigma[w(F_O^2)^2]\}^{1/2}$.

[c] $GOF= \{\Sigma[w(F_O^2-F_C^2)^2]/(n-p)\}^{1/2}$

Table 2

Comparison of crystallographic parameters from different oxaliplatin crystal structures.

Reference	[5]	[6]	This work	This work
Space group	$P2_1$	$P2_1/m$	$P2_1$	$P2_1/m$
Temperature, K	RT	120(2)	100(2)	100(2)
θ range, deg	1.8 – 22.5	2.74 – 26.00	1.82 – 29.60	1.82 – 29.60
Chirality	*R*,*R*	*rac*-(*R*,*R* + *S*, *S*)	*R*,*R*	*rac*-(*R*,*R* + *S*, *S*)
R1, %	4.0	1.92	1.11	1.22
wR2, %	5.3	5.20	2.71	3.27

Table 3

Crystallographic parameters for [Pt(*R*,*R*-DACH)I_2] ·DMF and *trans*-[Pt(*R*,*R*-DACH)(oxalate)$(OH)_2$] ·$3H_2O$

	[Pt(*R*,*R*-DACH)I_2] ·DMF	***trans*-[Pt(*R*,*R*-DACH)(oxalate)$(OH)_2$] ·$3H_2O$**
Formula	$C_6H_{14}I_2N_2Pt{\cdot}C_3H_7NO$	$C_8H_{16}N_2O_6Pt{\cdot}3(H_2O)$
Formula weight	636.18	485.37
Space group	P1	$P2_12_12_1$
a, Å	8.3973(4)	7.3994(3)
b, Å	10.1320(5)	8.9857(4)
c, Å	10.4594(5	22.4917(10)
α, °	72.4950(7)	
β, °	66.9200(6)	
γ, °	85.1034(7)	
V, $Å^3$	780.22(7)	1495.45(11)
Z	2	4
T, K	100(2)	100(2)
μ(Mo Kα), mm^{-1}	12.937	9.425
θ range, °	2.11 to 28.36	1.81 to 28.76
total no. of data	15189	30557
no. of unique data	7286	3854
no. of parameters	281	205
completeness to θ (%)	99.0	99.6
Flack *x*	0.027(6)	0.003(5)
$R_1{}^a$ (%)	1.78	1.15
$wR_2{}^b$ (%)	3.49	2.75
GOF[c]	0.997	1.097
max, min peaks, e $Å^{-3}$	1.37 and −0.91	0.76 and −0.64

[a] $R1=\Sigma||F_o| - |F_c||/ \Sigma|F_o|$.

[b] $wR_2= \{\Sigma[w(F_o{}^2-F_c{}^2)^2]/\Sigma[w(F_o{}^2)^2]\}^{1/2}$.

[c] $GOF= \{\Sigma[w(F_o{}^2-F_c{}^2)^2]/(n-p)\}^{1/2}$